International Journal of Innovative Research and Scientific Studies, 8(2) 2025, pages: 1684-1695

ISSN: 2617-6548

URL: www.ijirss.com

Modeling and optimization of slag for copper capturing of Platinum group metals from Al2O3-based concentrate

Erdenebold Urtnasan[1,2], Jei-Pil Wang[3*]

[1]*Industrial Science Technology Research Center, Pukyong National University, Busan 48513, Republic of Korea.*
[2]*Darkhan School of Technology, Mongolian University of Science and Technology, Darkhan city, Mongolia.*
[3]*Department of Metallurgical Engineering, BB21 plus team, Pukyong National University, Busan 48513, Korea.*

Corresponding author: Jei-Pil Wang (*Email: jpwang@pknu.ac.kr*)

Abstract

The mining of base metals, such as copper and nickel, frequently yields platinum group metals (PGMs) as byproducts, requiring specialized techniques for their extraction and purification. Platinum group metals (PGMs), found in concentrates with high aluminum oxide content, are associated within an aluminum oxide (Al_2O_3) matrix. The feasibility of dissolving platinum group metals (PGMs) in a metallic copper substrate was assessed through an investigation into the conversion of a platinum-bearing concentrate (72% aluminum oxide) to metallurgical slag. Within the $CaO–SiO_2–Al_2O_3$ partial equilibrium system, a thorough analysis was conducted to determine both the chemical composition and melting characteristics of the slag. Utilizing the Phase Diagram mode of Factsage software, a modeling of the slag structure at elevated temperatures was conducted, leading to the identification of an optimal slag composition exhibiting a reduced melting point. Based on the modeling conducted within the $CaO–SiO_2–Al_2O_3$ system, the optimal melting state of the slag was achieved at 1550 °C by fluxing with CaO and SiO_2 additions to reach a CaO/SiO_2 ratio of 0.7. The optimally melted slag, which was characterized by a CaO/SiO_2 ratio of 0.7, exhibited a morphology clearly indicative of the formation of an easily molten eutectic. A smelting experiment was conducted using 300 grams of concentrate, with the fluxing adjusted to a CaO/SiO_2 ratio of 0.7, successfully generating and maintaining a slag at a temperature of 1550 °C on a substrate of metallic copper. As a result, the copper matrix contained 111 mg/kg of Ag, 147 mg/kg of Pt, 213 mg/kg of Pd, and 204 mg/kg of Ir, a mix of PGMs.

Keywords: Concentrate based on alumina oxide, PGM-bearing concentrate, Platinum group metals dissolving, Slag modeling.

DOI: 10.53894/ijirss.v8i2.5528
Funding: This research is supported by Ministry of Science and ICT through the National Research Foundation of Korea (Brain Pool program with Grant number: RS-2023-00222959)
History: Received: 29 January 2025 / **Revised:** 4 March 2025 / **Accepted:** 11 March 2025 / **Published:** 20 March 2025

Competing Interests: The authors declare that they have no competing interests.
Authors' Contributions: Both authors contributed equally to the conception and design of the study. Both authors have read and agreed to the published version of the manuscript.
Transparency: The authors confirm that the manuscript is an honest, accurate, and transparent account of the study; that no vital features of the study have been omitted; and that any discrepancies from the study as planned have been explained. This study followed all ethical practices during writing.
Publisher: Innovative Research Publishing

1. Introduction

Platinum group metals (PGMs), including platinum (Pt), palladium (Pd), rhodium (Rh), ruthenium (Ru), iridium (Ir), and osmium (Os), are six noble, precious metals with similar chemical and physical properties, often found nestled together in the Earth's crust. The high density, impressive ductility, exceptional corrosion resistance, extremely high melting points, and remarkable catalytic properties inherent to these metals are critical to their applications in electronics, chemical production, aerospace, and automotive catalysis [1, 2]. The rarity of platinum group metals (PGMs) in the Earth's crust contributes to their exceptionally high and coveted market prices. Automotive demand has driven up their prices recently. The U.S. Geological Survey's data from the U.S. Geological Survey [3] and U.S. Geological Survey [4] reveals that global PGM reserves demonstrated significant growth, climbing to 81,000 metric tons by 2024, which represents a considerable increase of 12 metric tons compared to the reserve levels observed five years prior, underscoring a substantial surge in market demand. In 2024, South Africa dominated global PGM reserves, holding a staggering 88%, dwarfing Russia's 7.7%, Zimbabwe's 2.8%, and the combined 0.8% of others, including the U.S. and Canada [5, 6]. In nature, PGMs are found alongside copper (chalcopyrite, $CuFeS_2$), nickel (pentlandite, $(Fe,Ni)_3S_8$), and iron (pyrrhotite, $Fe_1{-}xS$) sulfide ores, their dark, heavy presence adding to the overall weight and density of the ore, with concentrations ranging from 2 to 10 g/t [7-9]. Although generally not the case, PGMs can be found in association with rocks exhibiting high aluminum oxide concentrations, a fact resulting in concentrates where the PGMs are associated within an Al_2O_3 mineral matrix. PGMs are precipitated as a sludge during the electro-refining process, in which copper and nickel are extracted from sulfide concentrates; this sludge is then further processed to separate and recover the individual PGMs. In contrast, the extensive use of high-alumina-based PGM concentrates in automotive and industrial catalysts is well-documented in the literature, as evidenced by the studies conducted by Grilli, et al. [10] and Dongfang, et al. [11]. The recovery of PGMs from alumina-based concentrates involves a range of techniques, from the high-temperature furnaces and chemical reactions of processing to the precise chemical dissolution of hydrometallurgical leaching and the unique biological processes of bioleaching. Several researchers, including [12-14], have shown that the choice of solution in hydrometallurgical processing is highly dependent on the specific PGM being treated, with common solutions being hydrochloric acid (HCl), nitric acid (HNO_3), sodium bisulfate ($NaHSO_4$), and aqua regia. Although hydrometallurgical methods boast impressive PGM recovery rates, their reliance on multiple, metal-specific leaching solutions, substantial reagent volumes, and significant environmental impact pose considerable limitations. Meanwhile, bioleaching is still largely confined to laboratory settings and small-scale trials, remaining a promising area of research. In high-temperature chlorination, PGMs react vigorously with chlorine gas and ammonium chloride (NH_4Cl), yielding metal chlorides including $PtCl_{4}/_{6}$, $PdCl_{2}/_{4}$, and $RhCl_{3}/_{6}$, creating a scene of intense heat and potentially hazardous fumes. The temperature for this procedure is typically set between 300 and 800 °C, depending on the specific properties of the chlorides [15-17]. Chlorination works well in smaller settings, but its limitations in scalability make it unsuitable for large industrial processes requiring high production volumes. High-alumina-based PGM concentrates are more effectively processed for mass production using pyrometallurgical methods, which form these concentrates into metallurgical slags characterized by their ease of melting and low viscosity. PGMs are extracted from this slag through co-melting with other metals or by allowing them to settle and then dissolving them into a metal substrate. The PGMs dissolving in metallic copper underwent enrichment in metallic copper at a smelting temperature between 1450 °C and 1600 °C, in a mild reducing or natural atmosphere. This process involved two distinct stages known as wetting and setting. A key principle in this technique is modeling the formation of a readily-meltable slag in the $CaO\text{-}Al_2O_3\text{-}SiO_2$ slag system, optimizing for fluidity and minimizing energy consumption. Several studies, including those conducted by Murata and Yamaguchi [18]; He, et al. [19] and Yan, et al. [20], suggest that incorporating Na_2O and B_2O_3 fluxes into metallurgical slags can facilitate improved metal settling due to the resultant reduction in slag melting point and the consequential improvement in slag fluidity. Introducing copper, iron, and lead into the slag causes these metals to combine with PGMs, forming a denser, heavier bi-metal phase that settles to the bottom of the slag, improving PGM recovery.

In Scheme 1, the process of transferring PGMs from molten slag into metallic copper is depicted through a mechanism in smelting. The small amounts of iron and copper present in the aluminum-based PGMs-bearing concentrate employed in this study serve a dual purpose: they allow for the reduction of these metals from the slag and enable their use as effective collectors for PGMs. The most efficient method for incorporating these PGMs is by dissolving them into a metallic copper substrate, thereby avoiding the mechanical losses to the slag. The process investigated in this study entails the chemical reaction of high-alumina concentrate with CaO and SiO_2 to yield a calcium aluminum silicate compound, identified as $CaAlSiO_x$. Due to the formation of this compound, a slag system is created which has a low viscosity and is easily meltable, thus allowing for the gravitational settling of platinum group metals such as platinum (density 21.45 g/cm^3), osmium (density 22.58 g/cm^3), and iridium (density 22.56 g/cm^3). The study's main objective is to comprehend the settling process, which involves a thorough investigation into the underlying principles of slag modelling. The presence of iron and copper in the concentrate, furthermore, acts to significantly enhance the collection of PGMs, thereby leading to an improvement in the overall recovery efficiency of the process.

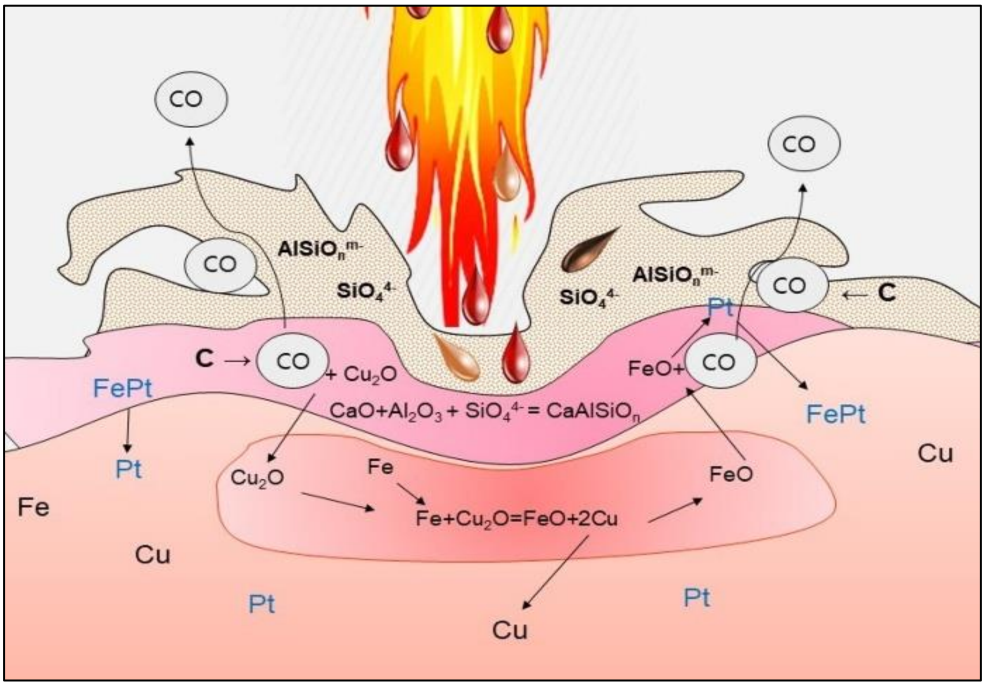

Figure 1.
Schematic diagram of the process platinum group metals (PGMs) transition from a slag into a copper matrix.

2. Materials and Methods

2.1. Experimental Materials

The platinum group metal (PGMs) concentrate underwent chemical composition analysis via XRF spectroscopy. The compositional analysis result is shown in Table 1. Aluminum oxide (Al_2O_3) constituted the predominant oxide component within the concentrate, comprising 72.24 wt.%. The principal constituents were 11.95 wt.% MgO, 3.23 wt.% CaO, and 3.17 wt.% SiO_2. Moreover, a 2.92 wt.% chlorine concentration was identified; this is likely due to residual flotation reagents. The concentrate included 0.21 wt.% CuO and 0.73 wt.% Fe_2O_3, elements with the potential to migrate from the molten slag to the metallic phase during smelting. High-purity quartz-form silicon dioxide (99.8%), sourced from Kanto Chemical Co., Inc., and extra-pure calcium oxide (96%), obtained from Samchun Chemical Co., Ltd., were used as the fluxing agents in this experiment. To prepare the copper substrate, high-purity copper powder, sourced from Duksan Pure Chemicals Co., Ltd., underwent a pre-melting process at a temperature of 1250°C within a controlled argon gas atmosphere.

Table 1.
The chemical composition of PGM-bearing concentrate analyzed by XRF.

Oxides	Al_2O_3	MgO	CaO	SiO_2	Cl	Na_2O	K_2O	TiO_2	Fe_2O_3	P_2O_5	CuO	ZnO	SO_3	Cr_2O_3	MnO
Wt.%	72.24	11.95	3.23	3.17	2.92	2.79	1.04	0.79	0.73	0.24	0.21	0.21	0.20	0.10	0.09

ICP-OES was used to analyze the PGM content in the concentrate. Silver and gold contents were measured and are reported in Table 2. There were 13 mg/kg of Ag and 50 mg/kg of Au present in the concentrate. Platinum and palladium were present at relatively low levels, 33 and 23 mg/kg respectively. The concentrate contained 200–400 mg/kg of Ir, Ru, and Os, considerably more than the platinum concentration. The economic efficiency of processing the concentrate could be significantly improved by these metals.

Table 2.
Platinum group metals in concentrate analyzed by ICP-OES.

Elements	Ag	Au	Pt	Pd	Ir	Ru	Os
mg/kg	13	50	33	23	323	433	181

The morphology and elemental distribution within the concentrate were determined by SEM-EDS analysis. Figure 2a (SEM image) shows the concentrate's irregular particle size and shape, including some agglomerated particles. An EDS mapping (Figure 2b) was used to examine the elemental distribution. Predominantly oxidized Al, Mg, and Na were observed in the EDS mapping, with the oxygen distribution confirming their oxidation state.

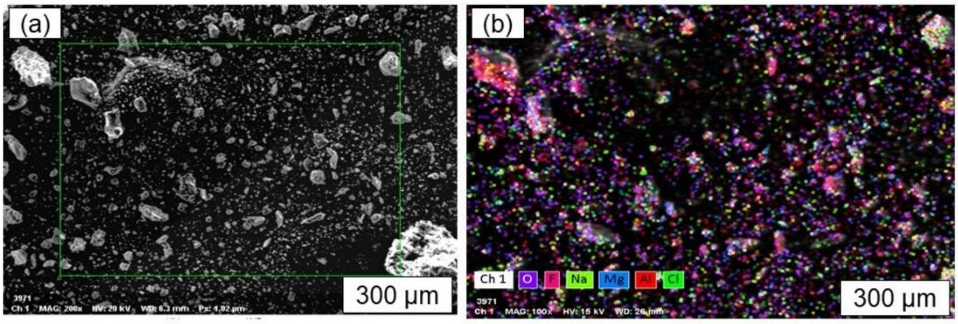

Figure 2.
SEM-EDS analysis of PGM concentrate; (a) SEM image and (b) EDS mapping.

Table 3 shows the EDS analysis results. The concentrate's composition, at 39.22 wt.% aluminum and 6.60 wt.% magnesium, confirms that these elements are its main constituents. This, along with the high oxygen levels, suggests that these elements are primarily in their oxidized states. The XRF analysis findings are supported by the EDS results; the concentrate mainly contains Al_2O_3, MgO, and CaO. The detected chlorine suggests that a significant quantity has been adsorbed onto the powder's surface.

Table 3.
The composition of PGM-bearing concentrate analyzed by EDS.

Oxides	**O**	**Al**	**Mg**	**Na**	**Cl**	**Ca**
Wt.%	44.86	39.22	6.60	3.50	3.08	2.74

X-ray diffraction (XRD) analysis was conducted to determine the mineralogical composition of the platinum group metal (PGM)-bearing concentrate. Corundum (Al_2O_3, PDF 01-074-1081) and aluminum oxide (AlO, PDF number 01-075-0278) were identified as the predominant phases. This observation aligns with the XRF analysis, revealing a substantial Al_2O_3 concentration within the concentrate. Spinel phases ($MgAl_2O_4$, PDF number 01-086-0084) were identified as significant impurities. Moreover, the presence of a small quantity of sodium aluminum oxide ($Na_2Al_{21}O_{34}$, PDF number 01-070-2487) was observed, indicating that the MgO and Na_2O previously identified by XRF analysis had reacted with the alumina to form secondary phases.

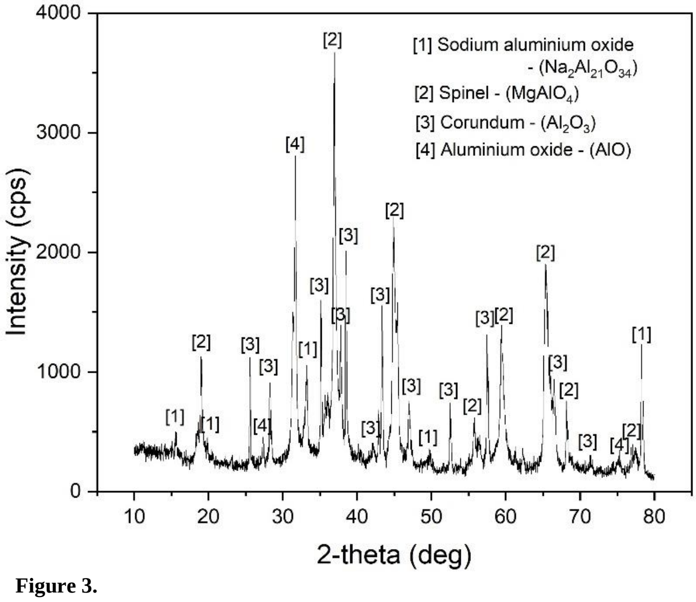

Figure 3.
XRD pattern of PGM-bearing concentrate.

2.2. Experimental Apparatus

The experimental process was divided into two key phases: firstly, a partial equilibrium study focusing on the transformation of the alumina-based concentrate into a readily fusible mass through melting; and secondly, a series of subsequent tests designed to effectively recover PGMs from this molten slag and dissolve them into copper. In order to convert the concentrate that contains PGMs into a low-melting slag, an equilibrium test was conducted in an argon atmosphere at a temperature of 1550 °C. The experimental apparatus is schematically illustrated in Figure 3. The smelting experiment occurred in a vertical tube, where the intense heat from molybdenum disilicide (MoSi2) elements reached a temperature of 1550 °C. The tube furnace, composed of a furnace controller and a heating box, stands tall with a B-type thermocouple inside. Inside the tube, there is a working space constructed from a 75 mm diameter alumina tube, with a length of 900 mm. With the ability to reach temperatures as high as 1800 °C, the tube furnace can be completely sealed off to prevent any air infiltration. Placed at the center of the working space, the sample was contained within an alumina crucible. To conduct the experiment, a carefully regulated stream of argon can be directed into the furnace. The thermocouple, with a high level of accuracy, was securely attached to the center zone of the furnace to closely monitor its operational temperature. By incorporating a temperature controlling system and programmable segments, the furnace grants users the ability to precisely adjust the heating rate, cooling rate, holding, and time settings. The experimental gas, under precise control from a mass flow controller (MFC), flowed into the furnace from one side. With a precision of ±2 cc, the fluid smoothly flowed through the working space at a controlled rate of 300 cc/min. Upon insertion of the sample into the furnace, the lid was closed tightly, and the furnace was filled with Ar gas. The sample in the furnace was slowly heated at a steady rate of 5 °C per minute until it reached 1550 °C, at which point it was left to hold. The sample was cooled down to room temperature at a rate of 5 °C per minute, without being removed from the furnace, and then it was taken out.

Utilizing an induction furnace, an experiment was conducted focusing on the recovery of PGMs from molten slag and their subsequent integration into copper. A 10 kW, 30 kHz high-frequency induction furnace was utilized to perform the dissolving smelting process, with a melt size of 10 kg of steel being processed within the furnace. The induction furnace included a cooler, controller, and heater. The smaller space led to miniaturized equipment (e.g., dust collector) to reduce costs. Voltage regulation controlled the temperature inside the high-frequency induction melting furnace. The heater box sealed the equipment, excluding dust and fumes. To create an inert atmosphere, argon gas was introduced into the heater box. Electricity flowed through the thermo-generator via graphite. As the crucible was heated, careful measurements of the temperature were taken.

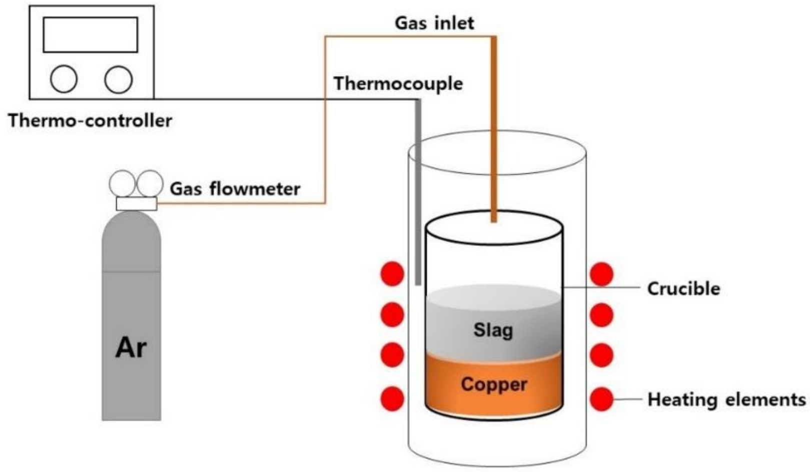

Figure 4.
Schematic diagram of experimental apparatus.

2.3. Analysis Methods

2.3.1. Thermodynamic Modelling

The software FactSage 8.2 was utilized for all thermodynamic modeling conducted within this research study. FactSage can compute equilibrium conditions for complex systems with numerous phases and chemical components, providing detailed insights into their interactions. Providing various output modes, such as tables and graphs, and possessing the ability to manage a wide range of constraints, it presents a robust and adaptable solution for data processing and visualization. In our study of the dissolution of PGMs during smelting, we employed the Equilib mode to ascertain the concentrations of the various chemical species present. The Equilib mode facilitated the optimization of flux addition to the concentrate, evaluation of homogeneous liquid slag formation, and determination of thermodynamic characteristics in slag smelting. In addition, the modeling of the slag composition was performed with the aid of the Phase Diagram module, which proved to be a valuable tool for this task. Utilizing the Phase Diagram module, the plot was calculated, which successfully captured the intricate details inherent within both ternary and multicomponent phase diagrams.

2.3.2. Chemical and Mineralogical Analysis

Employing a Shimadzu XRF-1800 model X-ray fluorescence spectrometer allowed for the determination of the chemical composition of the PGMs-bearing concentrate, a process that yielded highly accurate results. With careful attention to detail, the sample was placed inside a platinum crucible, which was then loaded into the XRF machine to begin the analysis process. In order to accurately measure the amounts of PGMs, a detailed analysis was carried out using the Agilent 5800 ICP-OES, a sophisticated Inductively Coupled Plasma Optical Emission Spectrometer. The mineral composition of the concentrate and slag was determined with the help of a high-intensity 3 kW Cu-Kα X-ray tube within an X-ray Diffractometer, specifically the model X'Pert-MPD PANalytical, which was instrumental in this process. In the XRD data acquisition process for the PGMs-bearing concentrate, a 10-minute scan was conducted over an angular range of 10 to 80 degrees, with incremental steps of 0.02 degrees used. X-ray fluorescence (XRF) spectroscopy, inductively coupled plasma optical emission spectrometry (ICP-OES), and X-ray diffraction (XRD) analyses were all conducted within the facilities of the Central

Laboratory located at Pukyong National University. The analysis in this study was conducted using the EM-30AX, which is a Scanning Electron Microscope and Energy Dispersive X-ray Spectrometer (SEM-EDS), allowing for a complete examination to determine the morphology and distribution of elements within the concentrate samples.

3. Results and Discussion

3.1. Thermodynamic modeling for the concentrate smelting into slag

In the process of smelting the alumina-based concentrate containing PGMs to form a slag in the $CaO-SiO_2-Al_2O_3$ system, the PGMs, due to their density difference with the surrounding mass, migrated downwards. The recovery of PGMs was facilitated by positioning a copper collector at the base of the slag, exploiting the principle that these metals dissolve into the copper from the molten slag. Utilizing the Factsage 8.2 software, a theoretical model was developed to represent this process. Slag formation from the PGMs-bearing concentrate was modeled using the Factsage software's Equilib mode, with material balance calculations based on the FactPS and FToxid databases applied under a standard atmospheric pressure of 1 atm. The melting characteristics of the concentrate, which comprises 72.24% Al_2O_3, 11.95% MgO, 3.23% CaO, and 3.17% SiO_2, were investigated over the temperature range spanning from 1300 to 1600 °C, providing valuable insight into its thermal properties. Figure 5a illustrates the relationship between the melting behavior of the concentrate and temperature, showing how the melting point changes as the temperature increases. Due to an insufficient amount of silicon dioxide, a primary structural component in metallurgical slags, calculations indicated that complete melting of the concentrate to form a fully molten metallurgical slag would be impossible. With the increase in temperature, the concentrate's constituent elements reacted to form various compounds, including those such as $CaMgAl_{16}O_{27}$ and refractory spinel phases like $MgAl_2O_4$ and $FeAl_2O_4$, among others. The formation of liquid slag and spinel phases showed a modest rise above 1500 °C, indicating a slight increase in their formation at higher temperatures. In the following calculation step, a CaO/SiO_2 ratio of 0.7 was used to add CaO and SiO_2 fluxes at 1550 °C, allowing for a model to be created that illustrates the effect this had on the melting behavior of the concentrate (Figure 5b). In the Equilib mode, the quantity of CaO flux introduced was treated as a variable that could be adjusted as needed. Upon reaching an addition amount of 30 grams, the flux readily reacted with the $CaMgAl_{16}O_{27}$ compound present within the concentrate, resulting in its transformation into a liquid slag. The computational models indicated that upon exceeding a flux addition of 50 grams, a complete conversion of the spinel phases to liquid slag occurred. In contrast to the expected results, a small quantity of the titanium-based spinel, specifically $MgTiAl_2O_5$, was observed during the calculation.

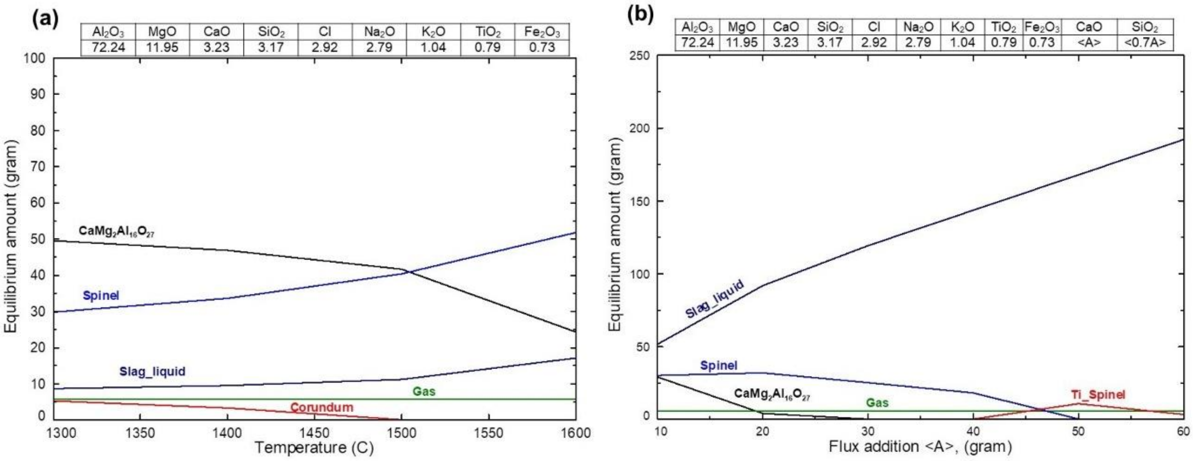

Figure 5.
Factsage Equilib calculations for PGMs-bearing concentrate smelting (a) at varying temperatures and (b) with flux addition at 1550 °C.

In order to transform the concentrate into slag, a thermodynamic analysis of the flux-added smelting process, conducted at a temperature of 1550 °C, was undertaken, utilizing the data generated by the Equilib mode as its basis. Figure 6a shows the relationship between the amount of flux added and the change in Gibbs free energy during smelting. Upon adding a flux of 10 grams, the Gibbs free energy was determined to be -2.1 MJ; however, when the amount of added flux increased to 50 grams, the Gibbs free energy value subsequently decreased to -3.3 MJ. This observation indicates that the main component of this concentrate, Al_2O_3, is changing its form into easily meltable eutectic compounds. The observation that the enthalpy of the reaction decreased as more flux was added confirmed that heat was released from the interaction between these oxides (Figure 6b).

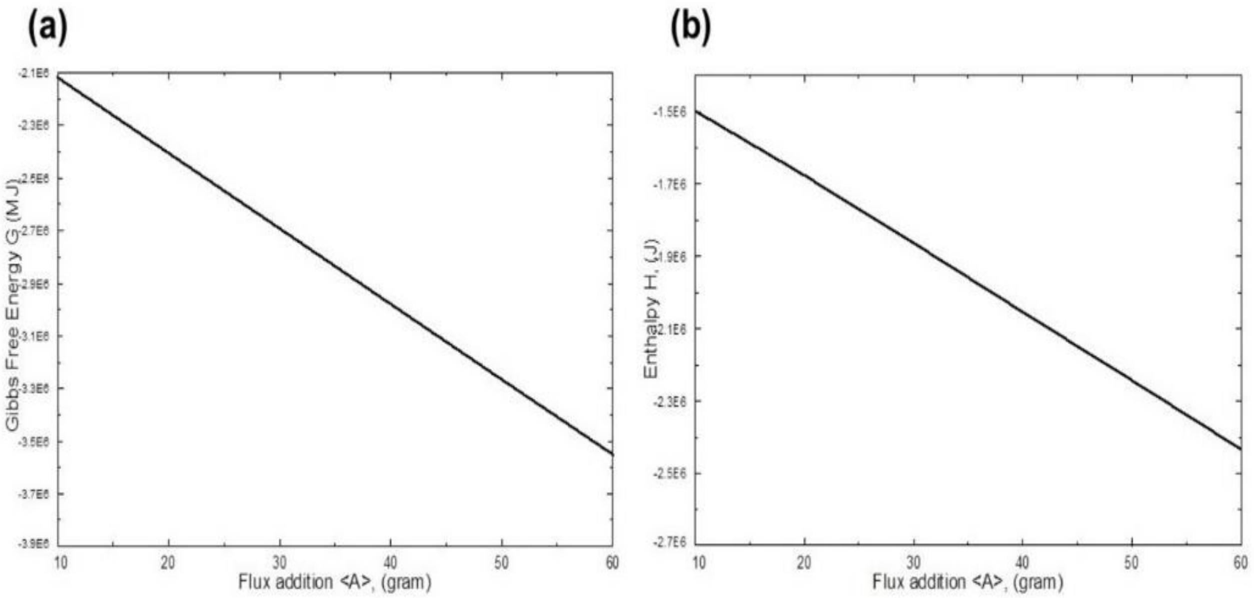

Figure 6.
Thermodynamic analysis of PGMs-bearing concentrate smelting with flux addition. (a) Gibbs free energy and (b) Heat of reaction in smelting.

When CaO and SiO_2 fluxes are added to the high-alumina concentrate that contains PGMs, high temperatures cause interactions between these oxides, resulting in the formation of eutectic compounds. Alumina silicates are formed from a combination of aluminum oxide (Al_2O_3) and silicon dioxide (SiO_2), while calcium silicates result from the reaction of calcium oxide (CaO) with silicon dioxide (SiO_2). Eutectic compounds are created through the interaction of aluminum oxide (Al_2O_3), calcium oxide (CaO), and silicon dioxide (SiO_2). The simplification of these interactions allows for their concise expression through Equations 1 to 4.

$$3Al_2O_3 + 2SiO_2 \rightarrow 3Al_2O_32SiO_2 \qquad (1)$$

$$CaO + Al_2O_3 \rightarrow CaOAl_2O_3 \qquad (2)$$

$$xCaO + ySiO_2 \rightarrow CaOSiO_2 / 3CaO2SiO_2 \qquad (3)$$

$$xAl_2O_3 + yCaO + nSiO_2 \rightarrow CaO\ Al_2O_32SiO_4 / 2CaO\ Al_2O_3SiO_2 \qquad (4)$$

Utilizing the Phase Diagram functionality within the Factsage software, a computational model was constructed to simulate the slag composition resulting from the processing of the platinum group metal-bearing concentrate; this model incorporated a temperature gradient and was based on the $CaO–SiO_2–Al_2O_3$ ternary system with an additional 10% MgO. Figure 8 shows the use of a ternary phase diagram to model the slag composition, a method that facilitated the determination of the slag melting temperature. Located in the Al_2O_3 region of the ternary phase diagram and labeled S0, the concentrate containing platinum group metals (PGMs) is a solid that remains in a non-molten state. Based on the Equilib mode calculations, for flux additions of 50 g, 60 g, and 70 g, respectively, the resulting slag structures consistently remain within the non-melting spinel phase regions, specifically the S1, S2, and S3 regions. The CaO/SiO_2 ratio for these slags approximates 1.4. In order to create a eutectic compound that melts easily at a temperature of 1500 °C, it is essential to lower the basicity of the slag and ensure that the slag's composition is within the range of molten $CaAl_2Si_2O_8$ slag. To reach this objective, it is necessary to modify the slag's basicity (CaO/SiO_2) by adjusting it to 0.5 for optimal results. This modification would result in a transition of the slag composition into the $CaAl_2Si_2O_8$ eutectic melt region, consequently enabling more facile melting at 1500 °C, as illustrated by the black circle in Figure 7.

3.2. PGMs-bearing concentrate smelting into slag

Based on the findings from our Equilib mode calculations, the simulated melting behavior of the slag, composed of $CaO–SiO_2–Al_2O_3$ with an additional 10% MgO, indicated that it resides within the solid spinel phase region of the system. A CaO/SiO_2 ratio exceeding unity yields a slag structure exhibiting a considerably elevated melting temperature, frequently characterized by increased viscosity and flow resistance. Conversely, a decrease in the CaO/SiO_2 ratio to below 0.5 can result in the formation of easily fusible slag, a significant alteration in the slag's properties. Due to a high concentration of Al_2O_3 in the $CaO–SiO_2–Al_2O_3$ ternary system, the slag's fluidity is significantly reduced, resulting in difficulties achieving complete melting of the slag. A key objective of this study, therefore, is the design of a slag system that achieves maximum Al_2O_3 content while maintaining its fusibility. With the goal of achieving the desired outcome, a series of flux-assisted melting experiments were designed and conducted at a temperature of 1550 °C, encompassing a range of CaO/SiO_2 ratios specifically 1.2, 0.7, and 0.3 to investigate the effect of varying these ratios on the melting process. Table 4 shows the quantities of CaO and SiO_2 flux additions used in these tests; the resulting slags, which were produced under varying CaO/SiO_2 ratios, are designated as labeled M1, M2, and M3, respectively. Considering the predicted compositions for each case, the primary constituents of the slag were computed based on partial equilibrium conditions within the $CaO–SiO_2–Al_2O_3$ system.

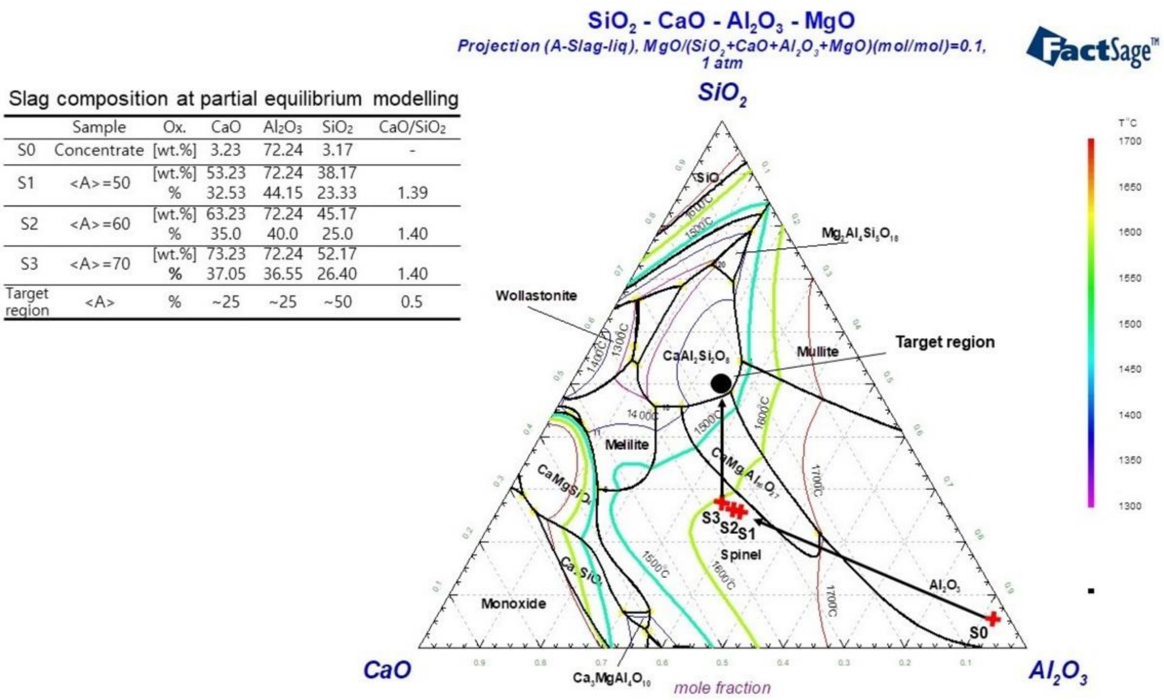

Slag composition at partial equilibrium modelling

	Sample	Ox.	CaO	Al_2O_3	SiO_2	CaO/SiO_2
S0	Concentrate	[wt.%]	3.23	72.24	3.17	-
S1	<A>=50	[wt.%]	53.23	72.24	38.17	
		%	32.53	44.15	23.33	1.39
S2	<A>=60	[wt.%]	63.23	72.24	45.17	
		%	35.0	40.0	25.0	1.40
S3	<A>=70	[wt.%]	73.23	72.24	52.17	
		%	37.05	36.55	26.40	1.40
Target region	<A>	%	~25	~25	~50	0.5

Figure 7.
Slag structure modeling at partial equilibrium in $CaO–SiO_2–Al_2O_3$ with 10% MgO system using projection diagram.

Table 4.
Input of flux addition for the PGMs-bearing concentrate smelting into slag.

Sample	Weight	Al_2O_3 in raw material	CaO	SiO_2	Mixture weight	CaO/SiO_2
M1	wt.%	72.24	56.27	46.9	203.17	1.2
	%	41.18	32.08	26.74		
M2	wt.%	72.24	52.44	73.9	226.3	0.7
	%	36.38	26.41	37.21		
M3	wt.%	72.24	41.78	154.8	296.53	0.3
	%	26.87	15.54	57.59		

Utilizing a flux-assisted smelting process, the experiment, which aimed to transform the platinum group metals-bearing concentrate into slag, was carried out at 1550 °C for a duration of 2 hours. The smelting process resulted in the formation of slag, and the chemical constituents of this slag are provided in Table 5. The slags that resulted from the smelting tests were labeled T1, T2, and T3 to correspond with the CaO/SiO_2 ratios used in each test. The experimental results confirmed the variation in the main slag components, which directly correlated with the amounts of flux added, precisely matching the pre-calculated CaO/SiO_2 ratios of 1.2, 0.70, and 0.3, as detailed and illustrated in Table 5. The results of the analysis of slag T1 showed that 34.33% was the CaO content, 27.33% was the SiO_2 content, and the Al_2O_3 content was determined to be 31.86%. Concurrently, there was a reduction in MgO content. Analysis of slag T1 revealed a CaO/SiO_2 ratio of 1.2, confirming that the target ratio established during the initial planning phase of the project had been successfully achieved. However, concerning slag types T2 and T3, the experimentally determined CaO/SiO_2 ratios deviated slightly from the initial design specifications, measuring 0.92 and 0.37, respectively.

Table 5.
The composition of slag formed from PGMs-bearing concentrate analyzed by XRF.

Sample	Oxides, %														
	SiO_2	Al_2O_3	CaO	MgO	Na_2O	Cl	K_2O	Fe_2O_3	CuO	TiO_2	Cr_2O_3	MnO	SO3	P_2O_5	C/S
T1	27.33	31.86	34.33	3.4	0.91	0.43	0.12	0.58	0.15	0.46	0.08	0.08	0.13	0.07	1.2
T2	32.08	29.57	29.63	3.89	1.54	1.59	0.49	0.43	0.10	0.34	0.06	0.06	0.06	0.06	0.92
T3	48.67	27.18	18.51	3.21	0.83	0.78	0.24	0.33	0.11	-	0.05	0.04	-	-	0.37

Considering the partial equilibrium conditions within the $CaO–SiO_2–Al_2O_3$ system, the compositions of slags T1, T2, and T3 underwent calculation, followed by an evaluation of their melting behavior at a temperature of 1550 °C. Figure 8 displays the predicted slag compositions (M1, M2, and M3), calculated and shown on a $CaO–SiO_2–Al_2O_3$ ternary diagram at a temperature of 1550 °C and a pressure of 1 atm, alongside the actual compositions obtained from melting experiments (T1, T2, and T3). While there are some small differences between the predicted compositions and those experimentally observed in the slags, all of the compositions still fall within the range where the slag is molten, successfully demonstrating that the desired slag formation conditions were achieved. The area marked with a red rhombus is where we predict the slag from the concentrate will be. It is clearly evident that the amount of Al_2O_3 found in this particular region demonstrates considerable fluctuation and inconsistency. Minimizing flux addition while simultaneously optimizing slag composition for ease of melting holds the potential for significant reductions in the energy costs associated with melting operations. Conversely, the minimal required flux addition observed in the M1 and T1 regions points to these compositions as the most economically favorable for slag formation. Numerous research studies have extensively investigated the correlation between the melting temperature and viscosity characteristics of slags within the $CaO–SiO_2–Al_2O_3$ system and their basicity. Research indicates that when basicity values are less than one, slags exhibit lower melting points and viscosities; these findings are consistent with prior research conducted by Liao, et al. [21]; Verun Deutscher Eisenhuttenleute (VDEh) [22] and Wang, et al. [23], all of which support the conclusion that slags exhibit lower melting points and viscosities when basicity values are less than one. According to Figure 8, it is evident that the movement of the slag composition toward the center of the liquid slag region is directly related to the basicity decreasing below a value of 1, as determined by the slag composition analysis. This observation indicates that a decrease in basicity is directly correlated with the formation of a slag structure that exhibits a lower melting point and thus is more easily melted.

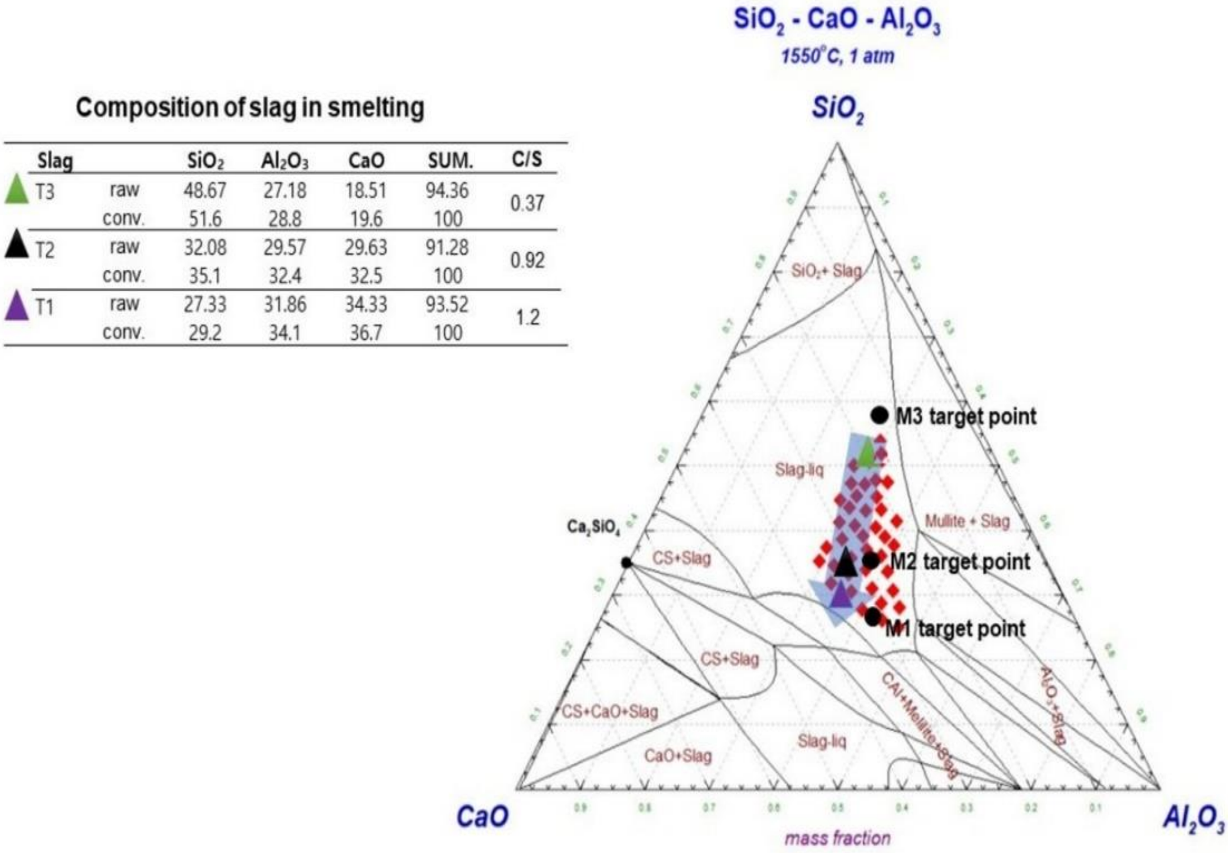

Composition of slag in smelting

Slag		SiO_2	Al_2O_3	CaO	SUM.	C/S
▲ T3	raw	48.67	27.18	18.51	94.36	0.37
	conv.	51.6	28.8	19.6	100	
▲ T2	raw	32.08	29.57	29.63	91.28	0.92
	conv.	35.1	32.4	32.5	100	
▲ T1	raw	27.33	31.86	34.33	93.52	1.2
	conv.	29.2	34.1	36.7	100	

Figure 8.
Slag melting analysis at partial equilibrium in $CaO–SiO_2–Al_2O_3$ system using Ftoxid data at 1550 °C.

A morphological examination conducted at 1550 °C of the T1, T2, and T3 slags, which were produced using different CaO/SiO2 ratios, clearly revealed distinguishable differences that were easily observable by visual inspection alone. Figure 8 shows images of the slags produced via flux addition melting at varying CaO/SiO2 ratios. The images on the right of Figure 9 depict the slags as they appeared after being melted inside the alumina crucible; in contrast, the left side provides magnified views that reveal the basic morphological structure of the slags. Characterized by porosity and incomplete melting, the T1 and T3 slags displayed a morphology indicative of their difficult and inefficient melting behavior. The T2 slag, however, displayed a significantly different structure; it was denser, contained fewer pores, and possessed a shiny appearance, all of which suggest that an easily molten eutectic was formed. As shown in Figure 8, the CaO–SiO2–Al2O3 phase diagram indicates that the T2 slag's position, which is notably distant from the crystallization curve and deeply within the liquid slag region, confirms its relatively favorable melting behavior. The results indicate that a more optimal and easily melted slag composition is potentially attainable at the specific CaO/SiO2 ratio under investigation.

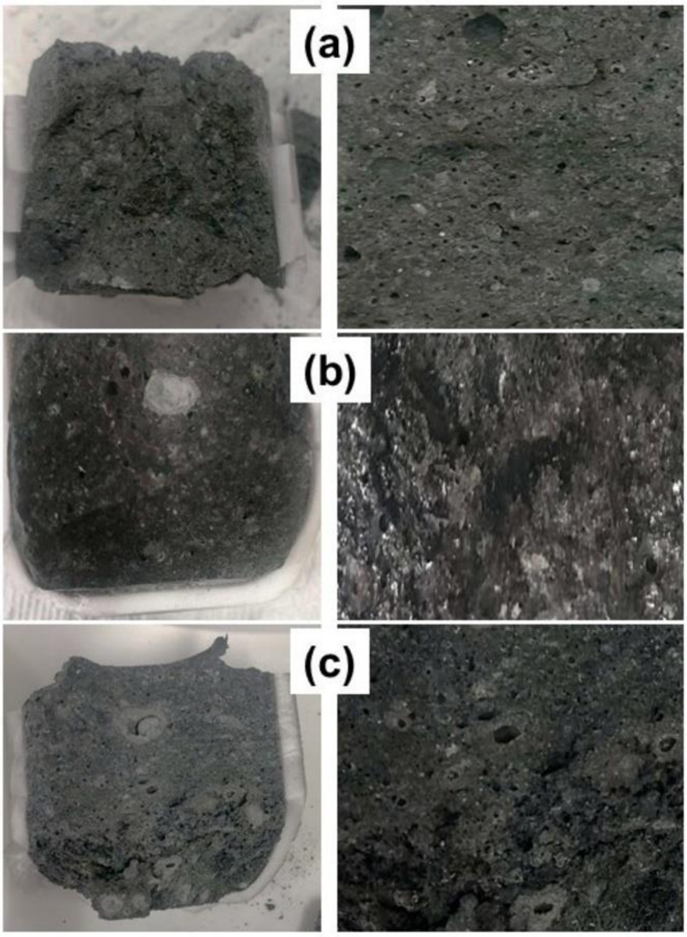

Figure 9.
Image of slag formed from PGMs-bearing concentrate on the ratio of CaO/SiO_2. (a) T3 slag with 1.2 ratio, (b) T2 slag with 0.9 ratio and (c) T1 slag with 0.37 ratio.

3.3. Smelting for PGMs dissolving in copper.

Utilizing partial equilibrium modeling within the CaO–SiO2–Al2O3 ternary system, the analysis confirmed that the slag possessing the T2 composition demonstrated relatively favorable melting characteristics at a temperature of 1550 °C. Following this, a melting experiment was performed to convert the PGM-bearing concentrate into a slag, with the goal of studying how much of the PGMs in the slag would dissolve in the copper substrate that was placed below the slag. In preparation for this experiment, a 300 g sample of the platinum group metal-containing concentrate was prepared; flux was then added to this sample to obtain a CaO/SiO2 ratio of 0.7, resulting in a homogeneous mixture. The test involved melting a sample at a high temperature of 1550 °C, where the sample was held at this temperature for a duration of 2 hours to ensure complete melting. A key objective of this experiment was to verify the hypothesis that PGMs could successfully transition from the molten slag to the copper substrate. Table 6 provides the chemical analysis of the slag resulting from the melting test. Upon comparing the new slag composition with the T2 slag composition presented in Table 5, several compositional differences were noted, specifically a 7% increase in SiO2 content, resulting in a final concentration of 39.33%, a slight 3% decrease in Al2O3 content to 26.51%, and a decrease of 0.1 in the CaO/SiO2 ratio, leading to a final ratio of 0.83. Although a minor alteration has been implemented, the CaO–SiO2–Al2O3 diagram shown in Figure 8 indicates that this adjustment does not substantially influence the melting characteristics of the slag, thus leading to the conclusion that the change is inconsequential. The slag analysis also showed 0.11% CuO; this indicates a small amount of copper from the substrate underwent oxidation and dissolved within the slag during the melting stage of the process. The observed interaction between the slag and the copper substrate confirms that the system can, in fact, facilitate the transfer of platinum group metals into the copper phase, thereby supporting the initial hypothesis.

XRF analysis was used to examine the composition of the slag produced during the smelting process of PGMs-bearing concentrate for PGMs extraction.

Table 6.
The composition of slag formed during the smelting process of PGMs-bearing concentrate for PGMs extraction, analyzed by XRF.

Oxide	SiO_2	CaO	Al_2O_3	MgO	Na_2O	Cl	K_2O	Fe_2O_3	CuO	TiO_2	SrO	C/S
%	39.33	29.83	26.51	2.89	0.45	0.28	0.11	0.15	0.11	0.25	0.03	0.83

Table 7 shows the chemical composition results of the copper substrate following the completion of the PGM dissolution test. Upon analysis of the high-purity copper sample, it was determined that contamination with iron, silicon, chlorine, aluminum, phosphorus, and chromium had occurred during the melting process. The contamination found is directly attributable to the graphite crucible used in the process, as it allowed for the reduction of elements from the slag and their subsequent transfer into the copper. Removing the impurities from this copper is easy; the process is quick and requires minimal effort. By introducing oxygen into the system, these elements can be effectively oxidized and returned to the slag phase in a straightforward manner. Through this process, the impurities are permitted to create stable oxides, which then move into the slag, resulting in the purification of the copper.

Table 7.
Composition of copper substrate analyzed by XRF.

Elements	**Cu**	**Si**	**Fe**	**Cl**	**Al**	**K**	**P**	**Cr**
Wt.%	94.01	4.30	0.55	0.40	0.38	0.14	0.10	0.07

ICP-OES analysis was employed to determine the content of PGMs in the copper substrate. Table 8 displays the contents of PGMs, expressed in milligrams per kilogram (mg/kg). Results showed successful dissolution, with the copper substrate containing significant traces of silver (111 mg/kg), platinum (147 mg/kg), palladium (213 mg/kg), and iridium (204 mg/kg). Unfortunately, the amounts of Au, Ru, and Os dissolving were not sufficient.

Table 8.
Platinum group metals in the copper substrate, by ICP-OES.

Elements	**Ag**	**Au**	**Pt**	**Pd**	**Ir**	**Ru**	**Os**
mg/kg	111	51	147	213	204	44	32

4. Conclusions

Due to its composition, which includes a high concentration of alumina minerals, the concentrate containing PGMs is known for its resistance to traditional smelting techniques and is therefore considered difficult to process. This study focused on the conversion of a high-alumina concentrate into a more easily meltable slag using the $CaO–SiO_2–Al_2O_3$ system, with a subsequent effort to extract PGMs from this slag using a copper substrate as the extraction medium. To investigate slag composition in the $CaO–SiO_2–Al_2O_3$ partial equilibrium system, CaO and SiO_2 fluxes were added to achieve CaO/SiO_2 ratios of 0.3, 0.7, and 1.2. To optimize this equilibrium system and achieve both reduced flux consumption and minimized melting energy usage, a strategy of maximizing the Al_2O_3 content is highly effective. The Factsage 8.2 software, specifically its Equilib and Phase diagram modes, provided the framework for creating a detailed model that accurately simulated the slag's melting characteristics. With a CaO/SiO_2 ratio below 0.7, the flux addition to the slag resulted in good melting behavior being observed at the high temperature of 1550 °C. An experiment was conducted in which 300 grams of concentrate, mixed with flux at a CaO/SiO_2 ratio of 0.7, was smelted on a high-purity copper substrate, resulting in the detection of the following concentrations of PGMs within the copper substrate: 111 mg/kg of Ag, 147 mg/kg of Pt, 213 mg/kg of Pd, and 204 mg/kg of Ir. In future research, the impact of the CaO/SiO_2 ratio, the duration of the melting process, and the temperature on PGMs recovery will be methodically investigated and determined.

References

[1] A. E. Hughes, N. Haque, S. A. Northey, and S. Giddey, "Platinum group metals: A review of resources, production and usage with a focus on catalysts," *Resources*, vol. 10, no. 9, p. 93, 2021. https://doi.org/10.3390/resources10090093

[2] S. Zhang, X. He, Y. Ding, Z. Shi, and B. Wu, "Supply and demand of platinum group metals and strategies for sustainable management," *Renewable and Sustainable Energy Reviews*, vol. 204, p. 114821, 2024. https://doi.org/10.1016/j.rser.2024.114821

[3] U.S. Geological Survey, "Mineral commodity summaries 2024," p. 212, 2024. https://doi.org/10.3133/mcs2024

[4] U.S. Geological Survey, "Mineral commodity summaries 2025," p. 212, 2025. https://doi.org/10.3133/mcs2025

[5] M.-P. Martínez-Hernando, E. García-Franco, D. Bolonio, M. F. Ortega, and M.-J. García-Martínez, "Life cycle sustainability assessment of the platinum supply chain in the European Union," *Sustainable Production and Consumption*, vol. 46, pp. 679-689, 2024. https://doi.org/10.1016/j.spc.2024.03.017

[6] F. Ríos Muñoz, C. Peña Ramírez, J. Meza, and T. Crouch, "Platinum Group Metals Extraction from Asteroids vs Earth: An Overview of the Industrial Ecosystems, Technologies and Risks: Mineral economics–raw materials report," *Mineral Economics*, vol. 37, no. 3, pp. 681-700, 2024. https://doi.org/10.1007/s13563-024-00429-y

[7] P. Sahu, M. Jena, N. R. Mandre, and R. Venugopal, "Platinum group elements mineralogy, beneficiation, and extraction practices–An overview," *Mineral Processing and Extractive Metallurgy Review*, vol. 42, no. 8, pp. 521-534, 2021. https://doi.org/10.1080/08827508.2020.1795848

[8] B. A. Gibson, G. Nwaila, M. Manzi, Y. Ghorbani, S. Ndlovu, and J. Petersen, "The valorisation of platinum group metals from flotation tailings: A review of challenges and opportunities," *Minerals Engineering*, vol. 201, p. 108216, 2023. https://doi.org/10.1016/j.mineng.2023.108216

[9] L. Qing-Lin, X.-Y. Song, T.-M. Long, R. Wirth, and Z.-H. Dai, "The effect of platinum-group minerals on differentiation of platinum-group elements in magmatic sulfide deposits: Evidence from the Cu-Ni-PGE deposits in the Yangliuping area of the Emeishan large igneous province, SW China," *Chemical Geology*, vol. 636, p. 121645, 2023. https://doi.org/10.1016/j.chemgeo.2023.121645.

[10] M. L. Grilli, A. E. Slobozeanu, C. Larosa, D. Paneva, I. Yakoumis, and Z. Cherkezova-Zheleva, "Platinum group metals: Green recovery from spent auto-catalysts and reuse in new catalysts—A review," *Crystals,* vol. 13, no. 4, p. 550, 2023. https://doi.org/10.3390/cryst13040550

[11] Y. Dongfang, Q. Yang, W. Ma, X. Ma, S. Wang, and Y. Lei, "Characteristics of spent automotive catalytic converters and their effects on recycling platinum-group-metals and rare-earth-elements," *Separation and Purification Technology,* vol. 308, p. 122977, 2023. https://doi.org/10.1016/j.seppur.2022.122977

[12] A. P. Paiva, F. V. Piedras, P. G. Rodrigues, and C. A. Nogueira, "Hydrometallurgical recovery of platinum-group metals from spent auto-catalysts–focus on leaching and solvent extraction," *Separation and Purification Technology,* vol. 286, p. 120474, 2022. https://doi.org/10.1016/j.seppur.2022.120474.

[13] S. Sun, C. Jin, W. He, G. Li, H. Zhu, and J. Huang, "A review on management of waste three-way catalysts and strategies for recovery of platinum group metals from them," *Journal of Environmental Management,* vol. 305, p. 114383, 2022. https://doi.org/10.1016/j.jenvman.2021.114383

[14] M. Niemelä, S. Pitkäaho, S. Ojala, R. Keiski, and P. Perämäki, "Microwave-assisted aqua regia digestion for determining platinum, palladium, rhodium and lead in catalyst materials," *Microchemical Journal,* vol. 101, pp. 75-79, 2012. https://doi.org/10.1016/j.microc.2011.11.001

[15] S. K. Padamata, A. S. Yasinskiy, and P. V. Polyakov, "Recovery of noble metals from spent catalysts. A review," *Metal and Material Transactions B,* vol. 51, pp. 2413-2435, 2020. https://doi.org/10.1007/s11663-020-01913-w

[16] Y.-k. Taninouchi, K. Sunagawa, T. H. Okabe, and H. Nakano, "Iron chloride vapor treatment for leaching platinum group metals from spent catalysts," *Journal of Sustainable Metallurgy,* vol. 10, no. 4, pp. 2227-2240, 2024. https://doi.org/10.1007/s40831-024-00910-6

[17] S. Kolbadinejad and A. Ghaemi, "Recovery and extraction of platinum from spent catalysts: A review," *Case Studies in Chemical and Environmental Engineering,* vol. 7, p. 100327, 2023. https://doi.org/10.1016/j.cscee.2023.100327

[18] T. Murata and K. Yamaguchi, "Recovery of palladium and platinum particles suspended in the Al2O3–CaO–SiO2 Slag using copper-based extractants at 1723 K," *Materials Transactions,* vol. 62, no. 10, pp. 1495-1501, 2021. https://doi.org/10.2320/matertrans.M-M2021844

[19] X.-F. He *et al.*, "Slag design and optimization for iron capturing platinum group metals from alumina-based spent catalysts," *Rare Metals,* vol. 42, no. 6, pp. 2093-2103, 2023. https://doi.org/10.1007/s12598-023-02262-8

[20] J. Yan *et al.*, "Comprehensive review on recovery of platinum group metals from spent automotive catalysts by metal capture technology: Present progress and outlook," *Journal of Environmental Chemical Engineering,* p. 114017, 2024. https://doi.org/10.1016/j.jece.2024.114017

[21] J. Liao, G. Qing, and B. Zhao, "Phase equilibrium studies of the CaO-MgO-Al2O3-SiO2 system for iron blast furnace slag: A review," *Metals,* vol. 13, no. 4, p. 801, 2023. https://doi.org/10.3390/met13040801

[22] Verun Deutscher Eisenhuttenleute (VDEh), *Slag Atlas*, 2nd ed. Dusseldorf: Verlag Stahleisen Gmbh, 1995.

[23] S. Wang *et al.*, "Effects of basicity and Al2O3 content on viscosity and crystallization behavior of super-high-alumina slag," *Crystals,* vol. 12, no. 6, p. 851, 2022. https://doi.org/10.3390/cryst12060851